Numerical Mass Balances for Cross Flow Membrane Contactors and Their Approximations

Sung Bin Park, Jung Woo Lee, Yong Soo Kim and Chul Soo Lee[†]

Department of Chemical and Biological Engineering, Korea University, Seoul 136-701, Korea
(*Received 6 December 2004 • accepted 22 March 2005*)

Abstract–Membrane contactor processes for stripping of sparingly soluble components such as oxygen are well understood. For readily soluble components in cross flow hollow fiber membrane modules, however, mass balances are less well established. In the present study, numerical and analytical solutions for cross flow modules are presented and compared with hitherto used solutions. Based on the comparison the best approximate solution is proposed.

Key words: Membrane Contactor, Cross Flow, Mass Transfer Coefficient, Mass Balance

INTRODUCTION

Membrane contactor processes are relatively new processes in which hollow fiber membrane modules provide an extensive interfacial area for phase contacts [Ho and Sirkar, 1992] and faster mass transfer [Yang and Cussler, 1986]. Unlike most membrane operations, the driving force for gas-liquid separation using membrane contactors is the chemical potential difference between gas and liquid phases rather than a pressure gradient [Gabelman and Hwang, 1999]. Other advantages and disadvantages in using membrane contactors have been discussed [Gabelman and Hwang, 1999; Reed et al., 1995]. Because the advantages of membrane contactors are often more important than the disadvantages, membrane contactors have attracted the attention of many interested groups in diverse applications [Gabelman and Hwang, 1999; Yagi et al., 1992].

In studies on stripping of sparingly soluble gases in membrane contactors, shell side flow rates of the stripped liquid phase are usually high and the concentration in the stripping phase is neglected, leading to a simple mass balance. In most studies, shell side flows were parallel with fibers [Yang and Cussler, 1986; Qi and Cussler, 1985a, b; Semmens et al., 1990; Choi et al., 2005]. The mass balance for parallel flows is further simplified by assuming plug flows in both shell and lumen sides. Later baffled modules were found to show better performance [Wang and Cussler, 1993]. The complex flow behavior of shell side flow in baffled modules has been analyzed assuming parallel or cross flow. Sengupta et al. [1998] and Schöner et al. [1998] used an approximate cross flow mass balance assuming that the concentration in the liquid phase changes only in radial directions and the concentration of stripped species in the stripping phase is negligible. Côté et al. [1989] applied the parallel flow model with non-negligible stripping phase concentration for the analysis of baffled cross flow modules. For readily soluble gases in a baffled module where the concentration of stripping phase is not negligible, a realistic mass balance model is yet to be developed.

In this study, a more general mass balance for cross flow modules is presented without assuming the negligible concentration of stripped species in gas phase. Also, numerical solutions are to be obtained for cross flow modules. Accuracies of analytic solutions are evaluated by comparing with numerical solutions and the best approximate solution is established.

MASS BALANCES FOR MEMBRANE MODULES

The mass balance of a membrane module for countercurrent parallel flows in a shell is given by Ho and Sirkar [Ho and Sirkar, 1992] and summarized here with different notations. Differential mass balance for lumen side gas flow and shell side liquid flow is

$$Q_g \frac{dC_{ig}}{dx} + Q_l \frac{dC_{il}}{dx} = 0 \tag{1}$$

where Qs are volumetric flow rates. The concentration changes due to mass transfer as represented by the mass transfer rate:

$$Q_g \frac{dC_{ig}}{dx} = \frac{AK_{il}}{L}(C_{il} - C_{ig}/H_i) \tag{2}$$

where A and L are the interfacial area and the effective length of a module, respectively. Henry's law is assumed for the partition coefficient of interfacial equilibria.

$$C_{ig} = H_i C_{il}^* \tag{3}$$

where the asterisk indicates the interfacial concentration of liquid phase in equilibrium with gas phase. Eqs. (1) and (2) are solved for the boundary conditions

$$C_{il} = C_{il}^0 \text{ at } x = 0; \ C_{ig} = C_{ig}^L \ \text{ at } x = L \tag{4}$$

to give the solution at the exit after some algebra

$$\frac{C_{il}^L}{C_{il}^0} = \frac{C_{il}^{out}}{C_{il}^{in}} = \frac{1 - R_Q}{\exp[K_Q(1 - R_Q)] - R_Q} + \frac{C_{ig}^L}{C_{il}^0 H_i} \frac{\exp[K_Q(1 - R_Q)] - 1}{\exp[K_Q(1 - R_Q)] - R_Q} \tag{5}$$

where

$$K_Q = K_{il}A/Q_l \text{ and } R_Q = -Q_l/Q_g H_i \tag{6}$$

For countercurrent flows Q_l and Q_g are of opposite sign and R_Q is a positive quantity.
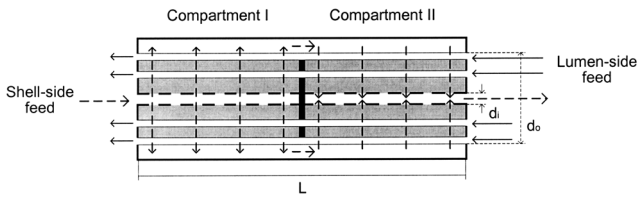
Fig. 1. Schematic view of membrane contactor module for cross flow in the shell side.

To derive the material balance for a cross flow in shell side and plug flow in lumen side of a hollow fiber membrane module as shown in Fig. 1, we first consider a cross flow module of length L without baffles. The gas flow in lumen side is assumed as plug flow whose concentration depends only on x,

$$Q_g \frac{dC_{ig}^x}{dx} + \frac{Q_l(R^2-R_0^2)}{2rL} \frac{\partial C_{il}(x,r)}{\partial r} = 0 \qquad (7)$$

where R $(=d_0/2)$ and $R_0 (=d_i/2)$ are outer and inner radii of the hollow fiber bundles in a module. In the derivation we used the continuity relation for the incompressible liquid phase,

$$2\pi r v_r L = \text{const} \qquad (8)$$

Integrating Eq. (7) with respect to r from R_0 to R at constant x and using the definition (6),

$$\frac{dC_{ig}^x}{dx} - \frac{R_Q H_i}{L}(C_{il}^R - C_i^{R_0}) = 0 \qquad (9)$$

The liquid phase concentration change due to mass transfer is also represented by an equation similar to Eq. (2).

$$\frac{(R^2-R_0^2)}{2r} \frac{\partial C_{il}}{\partial r} = -K_Q(C_{il} - C_{ig}/H_i) \qquad (10)$$

Integrating Eq. (10) with respect to r from R_0 to R at constant x,

$$C_{il}^R = (1-e^{-K_Q})C_{ig}^x/H_i + e^{-K_Q}C_i^{R_0} \qquad (11)$$

Eliminating C_i^R in Eq. (9) using Eq. (11) and integrating (9) with respect to x from x to L for the gas concentration at x, we have

$$\frac{C_{il}^{R_0}H_i - C_{ig}^x}{C_{il}^{R_0}H_i - C_{ig}^L} = \exp\left[R_Q(1-e^{-K_Q})\frac{x-L}{L}\right] \qquad (12)$$

For the outward liquid flow the concentration at R_0 is independent of x and equal to the input value at x=0. The value of C_{ig}^x in Eq. (12) is inserted in Eq. (11) to find C_{il}^R. The liquid phase concentration at x=L is an average value over x,

$$\frac{C_{il}^L}{C_{il}^{R_0}} = \frac{1}{L}\int_0^L \frac{C_{il}^R}{C_{il}^{R_0}}dx = 1 - \frac{1-F_1}{R_Q} + \frac{1-F_1}{R_Q}\frac{C_{ig}^L}{C_{il}^{R_0}H_i} \qquad (13)$$

where

$$F_1 = \exp[-R_Q(1-e^{-K_Q})] \qquad (14)$$

If the gas phase concentration is negligible, the integration of Eq. (9) yields C_i^R that is independent of x,

$$\frac{C_{il}^L}{C_{il}^{R_0}} = \frac{C_{il}^R}{C_i^{R_0}} = e^{-K_Q} + (1-e^{-K_Q})\frac{C_{ig}^L}{C_{il}^{R_0}H_i} \qquad (15)$$

which may also be obtained from Eq. (5) or (13) in the limit $R_Q \to 0$.

For the baffled module shown in Fig. 1 we need to apply the solution given by Eqs. (13) twice: once for x=0 to L/2 and once for x= L/2 to L.

$$\frac{C_{il}^L}{C_i^{R_0}} = \frac{(R_Q-1+F_{1/2})^2}{R_Q\{R_Q-(1-F_{1/2})^2\}} + \frac{R_Q(1-F_{1/2}^2)-(1-F_{1/2})^2}{R_Q\{R_Q-(1-F_{1/2})^2\}}\frac{C_{ig}^L}{C_{il}^{R_0}H_i} \qquad (16)$$

where

$$F_{1/2} = \exp[-R_Q(1-e^{-K_Q/2})] \qquad (17)$$

The concentration in gas phase is obtained from the integral mass balance,

$$C_{ig}^L - C_{ig}^0 = R_Q H_i(C_{il}^L - C_{il}^{R_0}) \qquad (18)$$

subject to the equilibrium constraint

$$C_{ig}^0/H_i \leq C_{il}^{R_0} \qquad (19)$$

The maximum fractions removed for fresh feed is obtained from Eqs. (18) and (19) for R_Q less than or equal to 1.

$$(C_{il}^{R_0} - C_{il}^L)/C_{il}^{R_0} = C_{ig}^0/C_{il}^{R_0}R_Q H_i \leq 1/R_Q \qquad (20)$$

To relax the assumption that C_{ig} is independent of r in the cross flow model, we consider a differential volume element from r to $r+\Delta r$ and from x to $x+\Delta x$. From the forward finite difference scheme for liquid flow, Eq. (10), and the backward difference scheme for gas flow, Eq. (7), we have the following equations:

$$C_{il}^{x,r+\Delta r} = C_{il}^{x,r} + K_Q \frac{\Delta r^2}{R^2-R_0^2}\left(\frac{C_{ig}^{x,r}}{H_i} - C_{il}^{x,r}\right) \qquad (21)$$

$$C_{ig}^{x-\Delta x,r} = C_{ig}^{x,r} - R_Q H_i\left(\frac{\Delta x R^2-R_0^2}{L}\frac{R^2-R_0^2}{\Delta r^2}\right)(C_{il}^{x,r+\Delta r} - C_{il}^{x,r}) \qquad (22)$$

The boundary conditions are

$$C_{ig}=C_{ig}^L \text{ at } x=L \text{ for } R_0\leq r\leq R; \ C_{il}=C_{il}^0 \text{ at } r=R_0 \text{ for all x} \qquad (23)$$

By adjusting $\Delta x/\Delta r^2$ depending on $R_Q H_i$ convergent solutions are obtained.

In the numerical scheme as well as in analytical models, the mass transfer coefficient was assumed independent of radial velocity. In gas-liquid membrane contactors, shell side liquid films generally control the mass transfer. In mass transfer correlations, Sherwood number is correlated as a function of Reynolds number, which is based on average radial velocity [Sengupta et al., 1998; Schöner et al., 1998; Côté et al., 1989; Jansen et al., 1994]. This implies that mass transfer coefficients depend on local velocity. This dependency can be incorporated in the numerical analysis by defining,

$$K_Q' = K_Q(v_r/<v_r>)^b \qquad (24)$$

and using this quantity instead of K_Q in Eq. (21). b is the power to which Reynolds number is raised in correlations. From Eq. (8) we have for the velocity ratio

$$\frac{v_r}{\langle v_r\rangle} = \frac{R_o-R_i}{r\ln(R_o/R_i)} \qquad (25)$$

and

$$r = (R_i^2 + j\Delta r^2)^{1/2} \qquad (26)$$

Table 1. Comparisons of fractions removed calculated by different methods

R_Q	K_Q	Numeric 1	Numeric 2	Cross 2	Parallel	Cross 4	Limit
5	10	.200	.200	.200	.200	.200	1.00
	5	.200	.200	.200	.200	.200	.993
	2	.200	.200	.200	.200	.200	.865
	1	.196	.196	.195	.197	.197	.632
	.5	.176	.175	.176	.178	.177	.393
	.2	.121	.119	.120	.121	.121	.181
1	10	.867	.864	.773	.909	.857	1.00
	5	.798	.795	.751	.833	.806	.993
	2	.649	.643	.638	.667	.659	.865
	1	.493	.486	.491	.500	.498	.632
	.5	.332	.323	.331	.333	.333	.393
	.2	.167	.163	.166	.167	.167	.181
.5	10	.986	.985	.932	.997	.985	1.00
	5	.937	.933	.904	.957	.944	.993
	2	.761	.755	.754	.775	.769	.865
	1	.560	.552	.559	.565	.563	.632
	.5	.361	.354	.361	.362	.362	.393
	.2	.174	.170	.174	.174	.174	.181
.1	10	1.00	1.00	.997	1.00	1.00	1.00
	5	.988	.986	.984	.990	.989	.993
	2	.846	.839	.844	.849	.848	.865
	1	.618	.608	.617	.619	.618	.632
	.5	.387	.379	.387	.387	.387	.393
	.2	.180	.176	.180	.180	.180	.181

where j indicates the jth radial cell.

RESULTS AND DISCUSSION

Eq. (16) is the solution based on the assumption that concentration of lumen flow is independent of radial position. To check the effect of the assumption on Eq. (16), numerical solutions were also obtained as described. Different solutions may be compared with the numerical solution as functions of two dimensionless groups, K_Q and R_Q, to assess the accuracy as shown in Table 1. In the table, Numeric 1 and Numeric 2 indicate the numerical solutions--the former for velocity independent K_Q and the latter for velocity dependent K_Q with the exponent b=1, which corresponds to the maximum in the literature correlations. Cross 2 and Cross 4 are cross flow solutions for two and four compartment solutions, respectively. The former is the cross flow analytical solution, Eq. (16), for baffled modules and the latter is obtained by iterative boundary matching using Cross 2 solution. Parallel and Limit denote the results of the parallel flow model, Eq. (5), and the limiting solution, Eq. (15). All solutions are independent of the partition coefficient when the input stripping gas is free from solute. K_Q is usually on the order of 1 to 10 for gas-liquid contactors.

Deviations from numerical solutions are summarized in Table 2. Close examination leads to the following general observations. The 'Limit' solution can be a good approximation for R_Q less than 0.1 as in the stripping of sparingly soluble gases. Parallel flow approximation is good if R_Q not in the vicinity of 1. Cross 2 solution is the

Table 2. Comparisons of different models with results of numerical analysis

R_Q	Deviations		Cross 2	Parallel	Cross 4	Limit
5	Dev1[#]	AAD%	.13	.29	.17	254
		MAX%	.83	1.11	.57	400
	Dev2[$]	AAD%	.43	.78	.66	255
		MAX%	.84	1.71	1.66	400
1	Dev1	AAD%	3.18	2.35	.84	21.5
		MAX%	10.8	4.38	1.01	24.4
	Dev2	AAD%	3.64	3.54	1.92	22.9
		MAX%	10.5	4.78	2.48	33.9
.5	Dev1	AAD%	1.72	1.01	.45	7.84
		MAX%	5.47	2.13	1.04	13.6
	Dev2	AAD%	2.32	2.22	1.61	9.15
		MAX%	5.38	2.58	2.26	14.5
.1	Dev1	AAD%	.19	.14	.08	1.27
		MAX%	.41	.35	.24	2.27
	Dev2	AAD%	1.16	1.28	1.22	2.45
		MAX%	2.11	2.11	2.11	3.95

[#]: Deviations from Numeric 1, [$]: deviations from Numeric 2

best approximation for R_Q greater than or equal to 5, but the range is probably not of practical importance. Cross 4 solution is generally the best solution regardless of R_Q and K_Q values. However, considering the experimental uncertainties in measuring the removal efficiency, the parallel flow model is probably acceptable. Lastly, the use of a velocity dependent mass transfer coefficient results in small increases of model deviations, which are acceptable.

CONCLUSIONS

The mass balance model for cross flow in shell side was derived for baffled membrane contactors without assuming infinitely dilute stripping phase. Numerical solutions were also obtained to establish the accuracies of various models. The cross flow solution for two baffled modules in series was found to provide the best approximation for cross flow baffled modules. However, the parallel flow solution was also found acceptable. The use of velocity dependent mass transfer coefficients was small. A valid range for the infinitely dilute stripping phase assumption was established in terms of dimensionless variables.

ACKNOWLEDGMENT

NOMENCLATURE

A : he interfacial area of a hollow fiber module [m^2]
C_i : concentration of component i [mol/m^3]
d_i : inside diameter of hollow fiber bundle [m]
d_o : outside diameter of hollow fiber bundle [m]
F_1 : defined by Eq. (14) [-]
$F_{1/2}$: defined by Eq. (17) [-]

H_i : partition coefficient of component i [-]
K_{il} : overall mass transfer coefficient of component i [m/s]
K_Q : defined by $K_Q=K_{il}A/Q_l$ [-]
L   : effective fiber length [m]
Q   : flow rate [m^3/s]
R   : outside radius of hollow fiber bundle [m]
R_0 : inside radius of hollow fiber bundle [m]
R_Q : defined by $R_Q=-Q_l/Q_gH_i$ [-]
T   : temperature [K]
V_l : liquid molar volume [m^{3}mol^{-1}]
v_r : linear velocity of liquid in the radial direction [m/s]

Superscripts
0   : position in a membrane module at x=0
L   : the position in a membrane module at x=L
x   : denote that the variable depends on only x
*   : interfacial state

Subscripts
g   : gas phase in lumen side
l : liquid phase in shell side

REFERENCES

Choi, S.-H., Gao, T. and Oh, S.-J., "A Study on the Absorption of Carbon Dioxide Using PVDF/Plasma Membrane Contactor," *Kor. Chem. Eng. Res.*, **43**, 161 (2005).

Côté, P., Bersillon, J.-L. and Huyard, A., "Bubble-free Aeration Using Membranes: Mass Transfer Analysis," *J. Membr. Sci.*, **47**, 91 (1989).

Gabelman, A. and Hwang, S.-T., "Hollow Fiber Membrane Contactors," *J. Membr. Sci.*, **159**, 61 (1999).

Ho, W. S. W. and Sirkar, K. K., *Membrane Handbook*, van Nostrand Reinhold, New York (1992).

Jansen, A. E., Klaasen, R., Feron, P. H. M., Hanemaaijer, J. H. and ter Meulen, B. Ph., *Membrane Gas Absorption Processes in Environmental Applications*, Membrane Process in Separation and Purification, Crespo, J. G. and Boddeker, K. W. eds., Kluwer Academic Publishers, Dordrecht (1994).

Qi, Z. and Cussler, E. L., "Hollow Fiber Gas Membranes," *AIChE J.*, **31**, 1548 (1985).

Qi, Z. and Cussler, E. L., "Microporous Hollow Fibers for Gas Absorption I. Mass Transfer in the Liquid," *J. Membr. Sci.*, **23**, 321 (1985).

Reed, B. W., Semmens, M. J. and Cussler, E. L., *Membrane Contactors*, Membrane separations technology. Principles and Applications, Nobel, R. D. and Stern, S. A., eds., Elsevier Science, Amsterdam (1995).

Schöner, P., Plucinski, P., Nitsch, W. and Daiminger, U., "Mass Transfer in the Shell Side of Cross Flow Hollow Fiber Modules," *Chem. Eng. Sci.*, **53**, 2319 (1998).

Semmens, M. J., Foster, D. M. and Cussler, E. L., "Ammonia Removal from Water Using Microporous Hollow Fibers," *J. Membr. Sci.*, **51**, 127 (1990).

Sengupta, A., Peterson, P. A., Miller, B. D., Schneider, J. and Fulk, Jr., C. W., "Large-scale Application of Membrane Contactors for Gas Transfer from or to Ultrapure Water," *Separation & Purification Tech.*, **14**, 189 (1998).

Wang, K. L. and Cussler, E. L., "Baffled Membrane Modules Made with Hollow Fiber Fabric," *J. Membr. Sci.*, **85**, 265 (1993).

Yagi, Y., Imaoka, Y., Kasama, Y. and Ohmi, T., "Advanced Ultrapure Water Systems with Low Dissolved Oxygen for Native Oxide Free Wafer Processing," *IEEE Trans. Semicond. Manufact.*, **2**, 5 (1992).

Yang, M.-C. and Cussler, E. L., "Designing Hollow-fiber Contactors," *AIChE J.*, **32**, 1910 (1986).